Journal of Applied Polymer Science

Characterization of the hydrogen bond in polyurethane/attapulgite nanocomposites

Yang Ti,[1] Qiang Wen,[2] Dajun Chen[1]

[1]State Key Laboratory for Modification of Chemical Fibers and Polymer Materials, College of Materials Science and Engineering, Donghua University, Shanghai 201620, China

[2]Synthetic Rubber Division of Sinopec Assets Management Corporation Baling Petrochemical

Correspondence to: D. Chen (E-mail: cdj@dhu.edu.cn)

ABSTRACT: In this article, thermoplastic polyurethane (TPU)/attapulgite (AT) nanocomposites were prepared by solution blending. The interaction between AT and TPU was investigated by Fourier transform infrared (FTIR) and dynamic mechanical analysis (DMA). The carbonyl stretching region (1680–1760 cm^{-1}) of infrared spectra was studied to investigate the difference of the hydrogen bonding degree of the samples. The degree of hydrogen-bonded carbonyl groups of the samples were found to be increased with increasing AT content and decreased with increasing temperature. The equilibrium between free and hydrogen-bonded carbonyl groups was discussed. The values of dissociation enthalpy of the hydrogen-bonded carbonyl groups increased with increasing AT content. Quantitative evaluations of the interaction between AT and TPU was conducted by analyzing the physical cross-links density of the samples. The results indicated that the physical cross-links density of the samples increased with increasing AT content. The results of tensile tests showed that with increasing AT content, the mechanical properties of the samples increased, which confirmed that strong interaction was formed between AT and TPU matrix. © 2015 Wiley Periodicals, Inc. J. Appl. Polym. Sci. **2016**, *133*, 43069.

KEYWORDS: clay; composites; polyurethanes

Received 15 June 2015; accepted 16 October 2015

DOI: 10.1002/app.43069

INTRODUCTION

Nanocomposites are a class of materials with unique chemical and physical properties and have wide applications in many areas. Dispersion of nanoscale inorganic fillers into organic polymers to enhance their physical properties has gained increasing interest in recent years.[1–5] Among all the nanocomposites, clay has attracted great attention.[6–10] Kuan *et al.*[7] prepared a saponite organoclay/waterborne polyurethane (WPU) nanocomposite. The mechanical properties of WPU increased with increasing clay content. Tien *et al.*[9] prepared montmorillonite/polyurethane (PU) by in situ polymerization. Compared with pristine PU, the thermal stability of the samples was found to be increased with the addition of montmorillonite.

Attapulgite (AT) is a natural hydrated magnesium–aluminum silicate clay consisting of a three-dimensional network of densely packed rods with a diameter less than 100 nm and a length ranging from hundreds of nanometers to several micrometers for each single rod. AT has been used as reinforcing fillers in many polymer matrixes include styrene butadiene rubber, polyvinyl alcohol, polyacrylonitrile, epoxy resins, etc.[11–15]

In our previous work,[16] waterborne polyurethanes (WPU), synthesized from poly(tetramethylene glycol), 4,4-diphenylmethane diisocyanate, and dimethylol butanoic acid were modified by blending of AT clay. The mechanical properties and thermal stability of WPU improved by the addition of AT.

Thermoplastic polyurethane (TPU) is another widely used material in daily life, such as in the fields of coatings, adhesives, fibers, foams, thermoplastic elastomers, etc.[17–21] In order to meet the requirement for different applications, modifications of TPU with improved physical properties are of great interest among researchers.[22–26]

In this work, AT was added into a polyether based TPU to prepare TPU/AT nanocomposites. The hydrogen bond between AT and TPU was investigated by Fourier transform infrared (FTIR) and dynamic mechanical analysis (DMA). The carbonyl stretching region in the FTIR spectra was concerned. With the method of curve fitting procedure, the difference of the degree of hydrogen-bonded carbonyl groups with increasing AT contents was investigated. The equilibrium between free and hydrogen-bonded carbonyl groups, the dissociation enthalpy and entropy

Additional Supporting Information may be found in the online version of this article.

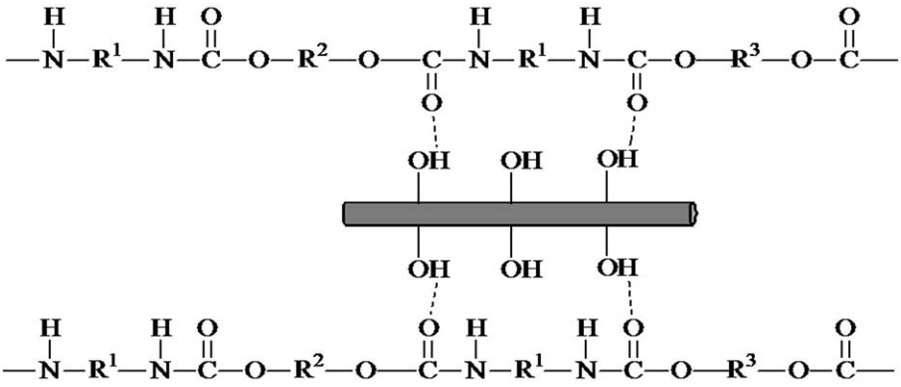

Scheme 1. Schematic of the possible dispersions of AT in TPU matrix.

of hydrogen-bonded carbonyl groups, and the physical cross-links density of the samples were discussed. The tensile tests of the samples were carried out to investigated the influence of the added AT on the mechanical properties of TPU.

EXPERIMENTAL

Materials

AT, purchased from Xuyu (China) and was purified in our lab, is a type of natural fibrillar clay with a theoretical half unit-cell formula $Mg_5Si_8O_{20}(OH)_2(OH_2)_4{\cdot}4H_2O$. The crude AT powder was pretreated with hydrogen peroxide solution and stirring with deionized water for 12 h. The resulting slurry was then diluted and gravitational sedimentated for 24 h to get rid of impurities. Then, the purified AT was treated in 1 mol/L hydrochloric (HCl) for 5 h to activate hydroxyl groups on AT surface and the suspension was separated through filtration, washed with deionized water until its pH value retained around 7 and then dried in vacuum at 70°C for 24 h. The structure and characterizations of the purified AT can be found in our previous works.[14,16,27,28] Dimethylacetamide (DMAc), with the water containing <100 ppm, was purchased from Shanghai Jingwei Chemical Co., China (Analytical Grade). Before used, DMAc was purified and further dehydrated by molecular sieves (0.4 nm) for more than two weeks. The PU sample (TPU 1180A) was obtained from BASF (commercial) and was used without further purified.

Sample Preparation

AT (0.1 g) was first dispersed in DMAc (100 g) under ultrasonic vibration (working frequency was at 53 KHz for 30 min). Then TPU (10 g) were added into the solution and stirred at 90°C for 3 h. The blending solutions were then casted on glass plates and placed in vacuum at 70°C for 3 days to remove the residual solvent. In this manner, four samples, with AT contents of 0, 1, 2, and 5 wt %, were prepared; they were named AT0, AT1, AT2, and AT5, respectively. The schematic of the possible dispersions of AT in TPU matrix is illustrated in Scheme 1.

Characterization

Scanning electron microscope (SEM) images of the cryo-fracture surfaces of the samples were taken with a SU8000 (Hitachi Co., Japan). The freeze-fractured surfaces of the SEM specimens were obtained in liquid nitrogen.

Infrared test was performed on a Nicolet 8700 infrared spectrophotometer and the spectra were recorded from 400 to 4000 cm^{-1} by averaging 64 scans at a resolution of 1 cm^{-1}. The films for infrared analysis were sufficient thin to be within the absorbance range where the Beer-Lambert law was obeyed. For the temperature scans, the samples were placed in a heating cell, which connected to a temperature controller. The temperature range was from 20 to 200°C with the control accuracy of ±0.1°C and the heating rate was about 10°C/min. The temperature of the sample was held constant for about 10 min before FTIR scan. Curve fitting procedure was carried out by using the software "OMNIC 7.5".

DMA data were obtained by a TA Q800 dynamic mechanical analyzer. The size of samples was about 11.0 mm×7.0 mm×0.30 mm. The tests were carried out from 30 to 90°C at a heating rate of 3°C/min with the frequency of 30 Hz and the vibration amplitude of 15 μm.

Tensile tests were performed on a universal material tensile machine (WDW3020, Changchun Greatwall Machine Co.) at 20°C. The size of the samples was about 60 mm×2 mm×0.08 mm. The initial length was set to be 30 mm and the crosshead speed was 200 mm/min. The results were averaged by at least five measured data.

RESULTS AND DISCUSSION

Morphology of TPU/AT Nanocomposites

SEM images of the fractured surfaces of AT0 and AT2 are shown in Figure 1. The fracture surface of AT0 was smooth, while that of AT2 showed many irregularly distributed nano-sized AT fibril. In addition, the interface between AT and the TPU matrix was not clear. Most AT fibrils were fractured and only a few fibrils were pulled out from the TPU matrix. It implied that the adhesion and dispersion between AT and TPU was good, which might be caused by the interaction between AT and TPU.

Infrared Analysis

The interaction can't be observed from the glass transition temperature (T_g) of the samples (supporting information Figure S1). In order to study the interaction, infrared analysis is utilized to investigate it for its high sensitivity to the change of hydrogen bond in TPU. The infrared spectra of the samples are shown in

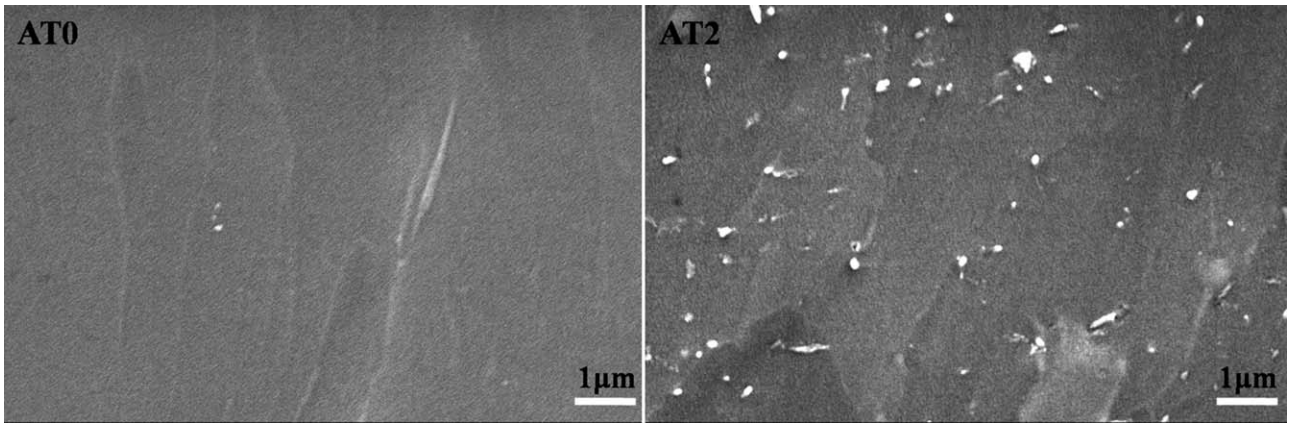

Figure 1. SEM images of fracture surfaces of AT0 and AT2. [Color figure can be viewed in the online issue, which is available at wileyonlinelibrary.com.]

Figure 2. The absorption bands at 3210–3460 cm^{-1} corresponded to the –NH stretching vibration, while the bands at 1680–1760 cm^{-1} corresponded to the carbonyl stretching vibration of TPU.[29] It is well known that TPU is an extensively hydrogen-bonded polymer.[30–32] Hydrogen bond in polyurethane can be characterized as a hard-hard segment hydrogen bond (NH- - - O=C bond) and a hard-soft segment hydrogen bond (NH- - - O– bond). The proton donor is –NH group of urethane, while the acceptor group is carbonyl and ester carbonyl or ether oxygen atom of urethane.[33] The carbonyl stretching vibration of TPU was concerned in this paper from where the fraction of hydrogen-bonded carbonyl groups could be calculated.[32–35] Two bands existed at the region from 1680 to 1760 cm^{-1} as shown in Figure 2 (labeled by frame). The sharp band centered near 1735 cm^{-1} was assigned to the stretching of free carbonyl groups, while the shoulder band centered near 1706 cm^{-1} was assigned to the stretching of hydrogen-bonded carbonyl groups.

The Fraction of Hydrogen-Bonded Carbonyl Groups at 20°C

According to Coleman,[34] the carbonyl stretching region is composed of free and hydrogen-bonded carbonyl groups. With the curve fitting procedure, the carbonyl stretching region of the samples can be curve fitted by two Gaussian bands, corresponding to the free and hydrogen-bonded carbonyl band near 1735 cm^{-1} and 1706 cm^{-1}, respectively.[32–35] The representative curve fitting results of the carbonyl stretching region of AT0 at 20°C is shown in Figure 3.

The ratio of absorption coefficients for free to hydrogen-bonded carbonyl band is 1.0.[32,35–37] X_b is defined as the fraction of hydrogen-bonded carbonyl groups and can be expressed by the following equation:

$$X_b = A_b/(A_b + A_f) \quad (1)$$

where A_f and A_b is the area of free and hydrogen-bonded carbonyl band, respectively.

The curve fitting results are listed in Table I. With increasing AT content, the fraction of hydrogen-bonded carbonyl increased. The results indicated that strong hydrogen bond was formed between AT and the hard segments of TPU. Similar phenomenon was reported in our earlier publications.[35,36] The possible mechanism of this interaction between AT and TPU might be that the additional hydrogen-bonded carbonyl groups are formed between free –C=O in TPU chain and –OH on the surface of AT.

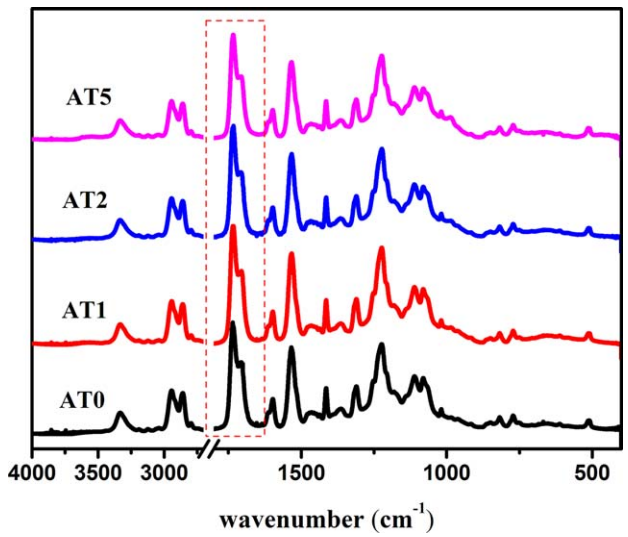

Figure 2. Infrared spectra of the samples at 20°C. [Color figure can be viewed in the online issue, which is available at wileyonlinelibrary.com.]

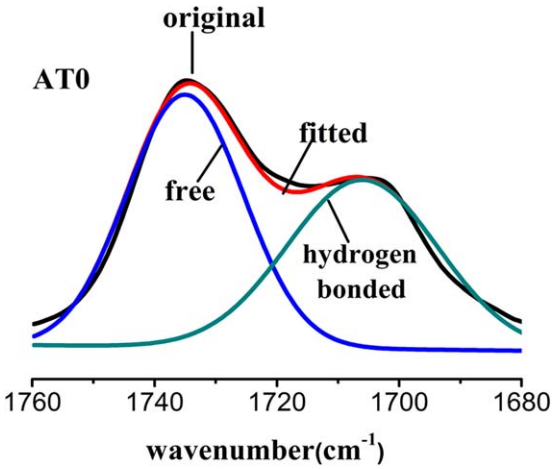

Figure 3. Curve fitting results in the carbonyl stretching region of the samples at 20°C. [Color figure can be viewed in the online issue, which is available at wileyonlinelibrary.com.]

Table I. Values of X_b at 20°C, ΔH_m, ΔS_m, and E_a of the Samples

Samples	X_b	ΔH_m (kJ/mol)	ΔS_m (J/mol K)	E_a (kJ/mol)
AT0	0.468	10.1	26.5	6.7
AT 1	0.486	10.5	27.7	7.3
AT 2	0.492	11.6	29.5	7.8
AT 5	0.500	11.8	29.6	10.6

Temperature Dependence of the Fraction of Hydrogen-Bonded Carbonyl Groups

To investigate the stability of the hydrogen bond formed between –OH of AT and the carbonyl groups of TPU, the temperature dependence of hydrogen-bonded carbonyl groups was studied. X_b of the samples as a function of temperature are shown in Figure 4. With increasing temperature, X_b of the samples containing AT remained a higher value than that of AT0. The results proved that the addition of AT increased the degree of hydrogen-bonded carbonyl groups of TPU. The formed hydrogen bond was stable and strong. It can also be found that with increasing temperature X_b decreased. It indicated a dissociation procedure, from hydrogen-bonded carbonyl groups to free carbonyl groups, existed.

As is shown in eq. (2), a dissociation balance exists between free and hydrogen-bonded carbonyl groups.

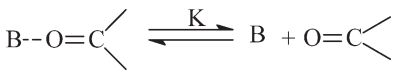

(2)

where B stands for –NH for AT0 sample, and –NH and –OH for AT1, AT2, and AT5 samples.

The equilibrium constant for the dissociation of hydrogen-bonded carbonyl can be determined by the following equation[38–40]:

$$K=[B][C=O]/[C=O\cdots B]=(1-X_b)^2/X_b \quad (3)$$

where K stands for the equilibrium constant; X_b is the fraction of hydrogen-bonded carbonyl groups.

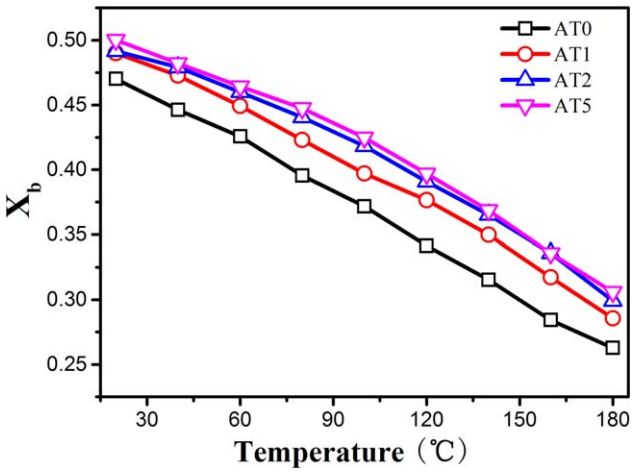

Figure 4. The fraction of hydrogen-bonded carbonyl groups of the samples as a function of temperature. [Color figure can be viewed in the online issue, which is available at wileyonlinelibrary.com.]

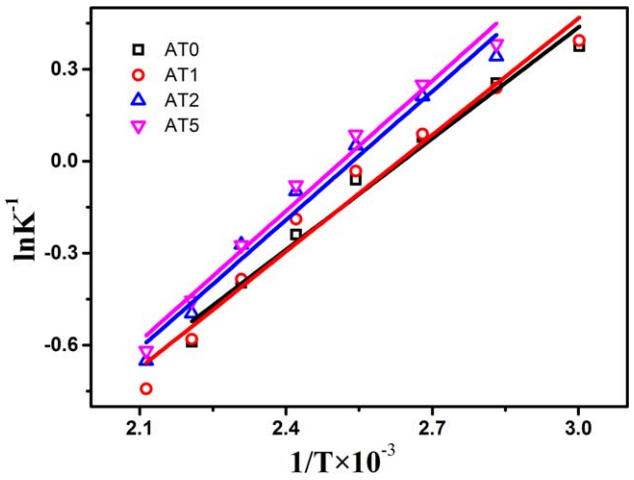

Figure 5. The data and linear fit of ln k^{-1} versus $1/T$ for the samples. [Color figure can be viewed in the online issue, which is available at wileyonlinelibrary.com.]

The temperature dependence of the equilibrium constant can be expressed by the following equation:

$$\ln K^{-1}=\Delta H_m/(RT)-\Delta S_m/R \quad (4)$$

The enthalpy (ΔH_m) and entropy (ΔS_m) for the dissociation of hydrogen bond were then calculated from eq. (4).

The data and linear fit of ln K^{-1} versus $1/T$ for the samples are shown in Figure 5. The values of ΔH_m and ΔS_m could be calculated from the slope and intercept and are summarized in Table I. The values of ΔH_m were increased with increasing AT content. It indicated that the dissociation of hydrogen bond in the samples containing AT needed higher energy than that in pure PU. The results supported that strong hydrogen bond was formed between AT and the hard segments of TPU. The degree of hydrogen-bonded carbonyl groups increased with increasing AT content.

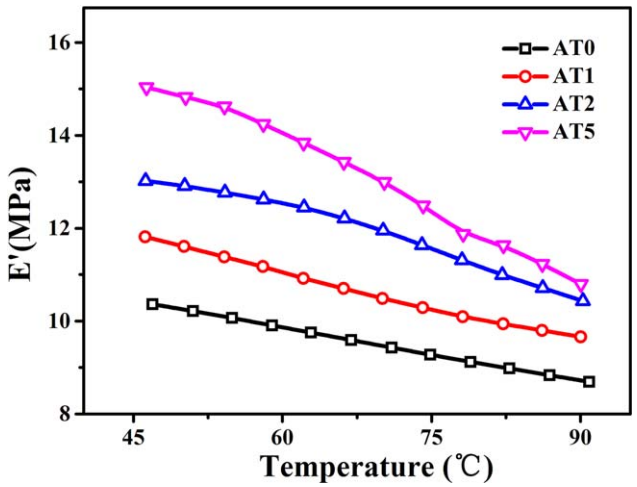

Figure 6. The storage modulus of the samples as a function of temperatures. [Color figure can be viewed in the online issue, which is available at wileyonlinelibrary.com.]

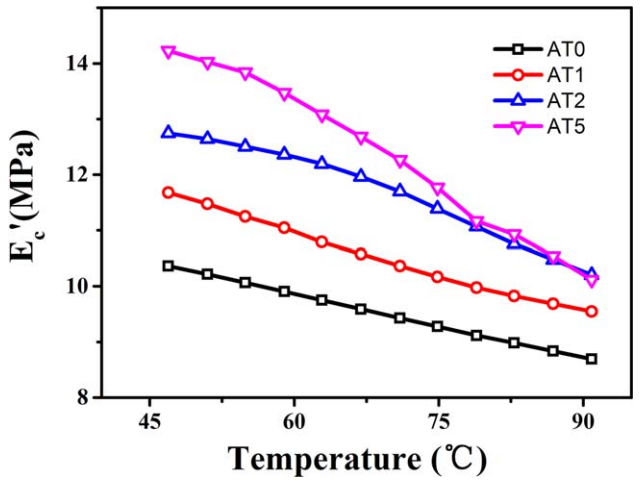

Figure 7. The corrected storage modulus of the samples as a function of temperatures. [Color figure can be viewed in the online issue, which is available at wileyonlinelibrary.com.]

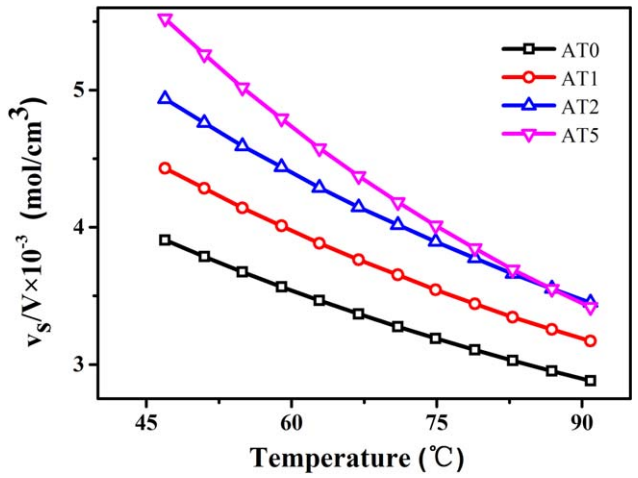

Figure 9. Effect of the temperature and the content of AT on the physical cross-linking density (v_s/V) of the samples. [Color figure can be viewed in the online issue, which is available at wileyonlinelibrary.com.]

Dissociation of Hydrogen Bond Investigated by Dynamic Mechanical Analysis

It is well known that the physical cross-links in TPU are mainly arisen from the hydrogen bond between the hard segments of TPU. Thus, the physical cross-links density in TPU can be used as a reflection to the fraction of the hydrogen bond in TPU. The storage modulus (E′) of the samples as a function of temperature is shown in Figure 6. It can be seen with increasing temperature, the storage modulus of the samples decrease, while with increasing AT content, the storage modulus of the samples increase. The influence of adding AT on the storage modulus can be divided into two parts. One is the interaction between AT and TPU matrix, which will increase the physical cross-links in TPU. The other is that AT is a rigid filler, the addition of which will increase the modulus. For a rigid filler/polymer system, the modulus of the composite can be described by Einstein's equation:

$$E_f = E_m\left(1+2.5V_f+14.2{V_f}^2\right) \quad (5)$$

where E_f is the modulus of the composite and E_m is the modulus of the matrix. V_f is the volume fraction of rigid filler, which can be estimated by following equation:

$V_f = \frac{m_{AT}/\rho_{AT}}{m_{PU}/\rho_{PU}+m_{AT}/\rho_{AT}}$, where m_{AT} and m_{PU} are the weight of AT and TPU, respectively; ρ_{AT} is about 2.1 g/cm^3;[41] and ρ_{PU} is about 1.1 g/cm^3.

Therefore, the corrected storage modulus of the sample can be obtained by following equation:

$$E'_c = E' - E_m\left(1+2.5V_f+14.2{V_f}^2\right) \quad (6)$$

where E'_c is the experimental value of storage modulus.

The corrected storage modulus of the samples as a function of temperatures is shown in Figure 7. Although the relationship between storage modulus and temperature shown in Figure 7 is similar to that shown in Figure 6, however, in this case only the interaction between AT and TPU matrix is involved.

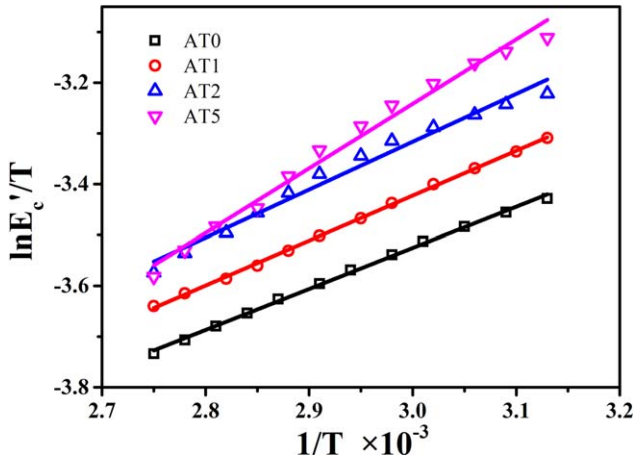

Figure 8. Plots of $\ln(E_c'/T)$ vs. $1/T$ for the samples. [Color figure can be viewed in the online issue, which is available at wileyonlinelibrary.com.]

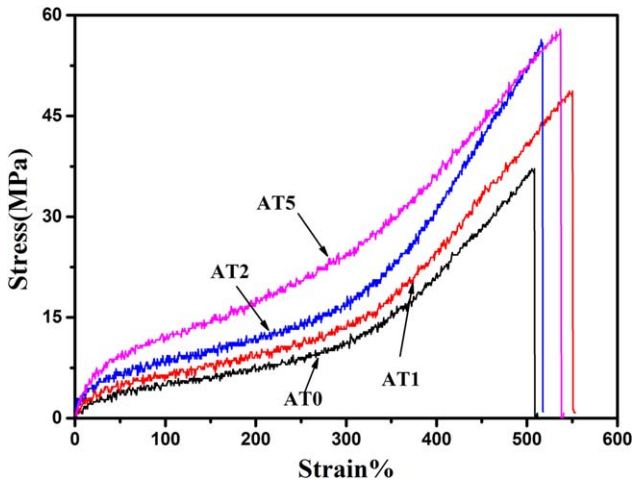

Figure 10. Strain–stress relations for the samples. [Color figure can be viewed in the online issue, which is available at wileyonlinelibrary.com.]

Table II. Mechanical Properties for the Samples

Sample	Tensile strength (MPa)	Elongation at break (%)
AT0	37.2 ± 1.7	527 ± 16
AT1	47.5 ± 2.2	568 ± 21
AT2	56.4 ± 2.3	520 ± 27
AT5	69.8 ± 5.1	537 ± 34

According to Weisfeld *et al.*,[42] the physical cross-linking density (v_s/V) can be expressed by the Arrhenius relationship:

$$v_s/V = A\exp(Ea/RT) \quad (7)$$

where A stands for a constant, R is the gas constant, T is the absolute temperature, and E_a is the activation energy of hydrogen bond dissociation.

For an elastomer, the measured storage modulus can be expressed as

$$E_c' = (v_s/V)RT \quad (8)$$

Using eqs. (7) and (8), eq. (9) can be obtained.

$$\ln(E_c'/T) = \ln(AR) + Ea/RT \quad (9)$$

Thus, E_a and A could be obtained from the slop and intersection of the straight line by plotting of $\ln(E_c'/T)$ versus $1/T$, as shown in Figure 8. By the addition of AT into TPU, the values of E_a were found to be increased. The result was listed in Table I. The trend of E_a was consistent with the trend of ΔH_m above, which indicated that the dissociation of hydrogen bond in the samples containing AT needed higher energy than that in pure TPU.

v_s/V could be calculated by eq. (7). The effect of the content of AT on the temperature dependence of v_s/V is shown in Figure 9. The values of v_s/V increased with increasing AT content. It indicated that the addition of AT increased the physical cross-linking density of TPU, which was consistent with the conclusion obtained above that rich hydrogen bond was formed between AT and the hard segments of TPU. Compared with X_b, the differences for the value of v_s/V of the samples were significant. Besides the hydrogen bond interaction, the physical cross-linking density of the samples may involve other interactions between AT and TPU, such as Van der Waals' interaction and so on. This may lead to the bigger differences between the values of v_s/V and X_b of the samples.

Mechanical Properties

Figure 10 shows the stress-strain curves for the samples. The corresponding tensile strength and the elongation at break of the samples are listed in Table II. It showed that with increasing AT content, the tensile strength of the samples increased significantly, from 37.2 to 69.8 MPa, while the elongation at break of the samples was almost the same. It indicated that the incorporation of AT improved the mechanical properties of PU and confirmed that strong interaction was formed between AT and PU.

CONCLUSION

In this paper, the interaction between AT and TPU in TPU/AT nanocomposites was investigated. With increasing AT content, hydrogen-bonded carbonyl groups increased. Strong hydrogen bond was formed between –OH of AT and the carbonyl groups of TPU. The values of ΔH_m of the hydrogen-bonded carbonyl groups for the samples increased from 10.1 to 11.8 KJ/mol with increasing AT content supported the conclusion. Quantitative evaluations of the interaction between AT and TPU showed that the physical cross-linking density of the samples increased with increasing AT content. The results of tensile tests showed that with increasing AT content, the mechanical properties of the samples increased.

ACKNOWLEDGMENTS

This work was supported by the Program of Introducing Talents of Discipline to Universities (No. 111-2-04).

REFERENCES

1. Akram, D.; Ahmad, S.; Sharmin, E.; Ahmad, S. *Macromol. Chem. Phys.* **2010**, *211*, 412.
2. Awad, S.; Chen, H.; Chen, G.; Gu, X.; Lee, J. L.; Abdel-Hady, E. E.; Jean, Y. C. *Macromolecules* **2011**, *44*, 29.
3. Chen, J.; Zhou, Y.; Nan, Q.; Ye, X.; Sun, Y.; Zhang, F.; Wang, Z. *Eur. Polym. J.* **2007**, *43*, 4151.
4. Gao, X.; Zhou, B.; Guo, Y.; Zhu, Y.; Chen, X.; Zheng, Y.; Gao, W.; Ma, X.; Wang, Z. *Colloid. Surface Physicochem. Eng. Aspects* **2010**, *371*, 1.
5. Wang, T.; Yang, C.; Shieh, Y.; Yeh, A. *Eur. Polym. J.* **2009**, *45*, 387.
6. Dan, C.; Lee, M. H.; Kim, Y. D.; Min, B. H.; Kim, J. H. *Polymer* **2006**, *47*, 6718.
7. Kuan, H.; Ma, C. M.; Chuang, W.; Su, H. *J. Polym. Sci. Pol. Phys.* **2005**, *43*, 1.
8. Pavličević, J.; Špírková, M.; Jovičić, M.; Bera, O.; Poręba, R.; Budinski-Simendić, J. *Compos. B* **2013**, *45*, 232.
9. Tien, Y.; Wei, K. *J. Appl. Polym. Sci.* **2002**, *86*, 1741.
10. Xu, B.; Huang, W. M.; Pei, Y. T.; Chen, Z. G.; Kraft, A.; Reuben, R.; Hosson, J.; Th., M.; De., Fu, Y. Q. *Eur. Polym. J.* **2009**, *45*, 1904.
11. Tian, M.; Qu, C.; Feng, Y.; Zhang, L. *J. Mater. Sci.* **2003**, *38*, 4917.
12. Wang, F.; Wang, H.; Zheng, K.; Chen, L.; Zhang, X.; Tian, X. Y. *Colloid. Polym. Sci.* **2014**, *292*, 953.
13. Chen, Y.; Zhou, S.; Gu, G.; Wu, L. *Polymer* **2006**, *47*, 1640.
14. Yin, H.; Chen, H.; Chen, D. *J. Mater. Sci.* **2010**, *45*, 2372.
15. Zhang, Y.; Shen, J.; Xu, Z.; Yeung, K. W. K.; Yi, C.; Zhang, Q. *Polym. Compos.* **2014**, *35*, 86.
16. Pan, H.; Chen, D. *Eur. Polym. J.* **2007**, *43*, 3766.
17. Ashhari, S.; Sarabi, A. A.; Kasiriha, S.; Zaarei, D. *J. Appl. Polym. Sci.* **2011**, *119*, 523.
18. Barick, A. K.; Tripathy, D. *Polym. Adv. Technol.* **2010**, *21*, 835.
19. Jin, H.; Wie, J.; Kim, S. *J. Appl. Polym. Sci.* **2010**, *117*, 2090.
20. Kotal, M.; Srivastava, S.; Bhowmick, A.; Chakraborty, S. *Polym. Int.* **2011**, *60*, 772.

21. Mishra, A. K.; Narayan, R.; Raju, K.; Aminabhavi, T. M. *Prog. Org. Coat.* **2002**, *74*, 134.
22. Bandarian, M.; Shojaei, A.; Rashidi, A. *Polym. Int.* **2011**, *60*, 475.
23. Cai, D.; Jin, J.; Yusoh, K.; Rafiq, R.; Song, M. *Compos. Sci. Technol.* **2012**, *72*, 702.
24. Fiorio, R.; Zattera, A.; Ferreira, C. *Polym. Eng. Sci.* **2010**, *50*, 2321.
25. Gireesh, K.; Allauddin, K.; Radhika, K.; Narayan, R.; Raju, K. *Prog. Org. Coat* **2010**, *68*, 165.
26. Verdolotti, L.; Colini, S.; Porta, G.; Iannace, S. *Polym. Eng. Sci.* **2011**, *51*, 1137.
27. Fang, Y.; Chen, D. *Mater. Res. Bull.* **2010**, *45*, 1728.
28. Lin, Q.; Gu, Y.; Chen, D. *J. Appl. Polym. Sci.* **2013**, *129*, 2571.
29. Coleman, M. M.; Skrovanek, D. J.; Hu, J.; Painter, P. C. *Macromolecules* **1988**, *21*, 59.
30. Mattia, J.; Painter, P. *Macromolecules* **2007**, *40*, 1546.
31. Seymour, R. W.; Cooper, S. L. *Macromolecules* **1973**, *6*, 48.
32. Teo, L. S.; Chen, C. Y.; Kuo, J. F. *Macromolecules* **1997**, *30*, 1793.
33. Brunette, C. M.; Hsu, S. L.; MacKnight, W. *J. Macromolecules* **1982**, *15*, 71.
34. Coleman, M. M.; Lee, K. H.; Skrovanek, D. J.; Painter, P. C. *Macromolecules* **1986**, *19*, 2149.
35. Ti, Y.; Chen, D. *J. Appl. Polym. Sci.* **2013**, *130*, 2265.
36. Ti, Y.; Chen, D. *Prog. Org. Coat.* **2012**, *76*, 119.
37. Ti, Y.; Lv, Y.; Chen, D. *J. Polym. Res.* **2014**, *21*, 1
38. Chen, S.; Hu, J.; Zhuo, H.; Yuen, C.; Chan, L. *Polymer* **2010**, *51*, 240.
39. Ning, L.; Ning, W.; Kang, Y. *Polymer* **1996**, *37*, 3577.
40. Shen, D. Y.; Pollack, S. K.; Hsu, S. L. *Macromolecules* **1989**, *22*, 2564.
41. Marshall, C. E.; Caldwell, O. G. *J. Phys. Colloid. Chem.* **1947**, *51*, 311.
42. Weisfeld, L. B.; Little, J. R.; Wolstenbolme, W. E. *J. Polym. Sci.* **1962**, *56*, 455.